Published in final edited form as:
*Clin Cancer Res*. 2012 February 1; 18(3): 726–736. doi:10.1158/1078-0432.CCR-11-2521.

# Activation of Beta-Catenin Signaling in Androgen Receptor–Negative Prostate Cancer Cells

**Xinhai Wan**[1], **Jie Liu**[1], **Jing-Fang Lu**[1], **Vassiliki Tzelepi**[1,2], **Jun Yang**[1], **Michael W. Starbuck**[1], **Lixia Diao**[3], **Jing Wang**[3], **Eleni Efstathiou**[1,4], **Elba S. Vazquez**[5], **Patricia Troncoso**[6], **Sankar N. Maity**[1,*], and **Nora M. Navone**[1,*]

[1]Department of Genitourinary Medical Oncology, The University of Texas MD Anderson Cancer Center, Houston, Texas

[2]Department of Pathology, University of Patras, Patras, Greece

[3]Department of Bioinformatics and Computational Biology, The University of Texas MD Anderson Cancer Center, Houston, Texas

[4]Department of Clinical Therapeutics, University of Athens, Athens, Greece

[5]Departament de Biological Chemistry, School of Sciences, University of Buenos Aires, CONICET, Buenos Aires, Argentina

[6]Department of Pathology, The University of Texas MD Anderson Cancer Center, Houston, Texas

## Abstract

**Purpose—**To study Wnt/beta-catenin in castrate-resistant prostate cancer (CRPC) and understand its function independently of the beta-catenin–androgen receptor (AR) interaction.

**Experimental Design—**We performed beta-catenin immunocytochemical analysis, evaluated TOP-flash reporter activity (a *reporter* of beta-catenin–mediated transcription), and sequenced the beta-catenin gene in MDA PCa 118a, MDA PCa 118b, MDA PCa 2b, and PC-3 prostate cancer (PCa) cells. We knocked down beta-catenin in AR-negative MDA PCa 118b cells and performed comparative gene-array analysis. We also immunohistochemically analyzed beta-catenin and AR in 27 bone metastases of human CRPCs.

**Results—**Beta-catenin nuclear accumulation and TOP-flash reporter activity were high in MDA PCa 118b but not in MDA PCa 2b or PC-3 cells. MDA PCa 118a and 118b cells carry a mutated beta-catenin at codon 32 (D32G). Ten genes were expressed differently (false discovery rate, 0.05) in MDA PCa 118b cells with downregulated beta-catenin. One such gene, hyaluronan synthase 2 (*HAS2*), synthesizes hyaluronan, a core component of the extracellular matrix. We confirmed HAS2 upregulation in PC-3 cells transfected with D32G-mutant beta-catenin. Finally, we found nuclear localization of beta-catenin in 10 of 27 human tissue specimens; this localization was inversely associated with AR expression ($P = 0.056$, Fisher's exact test), suggesting that reduced AR expression enables Wnt/beta-catenin signaling.

Corresponding Author: Nora M. Navone, Department of Genitourinary Medical Oncology–Research, Unit 18-6, The University of Texas MD Anderson Cancer Center, 1515 Holcombe Boulevard, Houston, TX 77030-4009. Phone: 713-563-7273; Fax: 713-745-9880; nnavone@mdanderson.org.
[*]Nora M. Navone and Sankar N. Maity contributed equally to this work.
Current address for J. Liu: Saint Mary's Hospital, 56 Franklin St., Waterbury, CT 06706.

**Disclosure of Potential Conflicts of interest**
No potential conflicts of interest exist.

**Conclusion—**We identified a previously unknown downstream target of beta-catenin, HAS2, in PCa, and found that high beta-catenin nuclear localization and low or no AR expression may define a subpopulation of men with bone-metastatic PCa. These findings may guide physicians in managing these patients.

### Keywords

beta-catenin; prostate cancer; androgen receptor; hyaluronan synthase

## Introduction

Recent reports have indicated that androgen receptor (AR)–mediated mechanisms are central to the castrate-resistant progression of prostate cancer (PCa) from localized to bone-metastatic disease (1–3), although multiple pathways likely cooperate to drive its growth at this advanced stage.

We recently developed 2 xenograft models, MDA PCa 118a and MDA PCa 118b, that were derived from 2 bone metastases in a man who had castrate-resistant PCa (CRPC) with widespread osteoblastic metastases (4). The cancer cells in these xenografts, like those in the human tumors of origin, do not express AR and can grow in castrated male mice. As such, they can be used to identify AR-independent mechanisms of castrate-resistant progression that likely would define a subtype of PCas. It is also likely that the same mechanisms play an important, albeit more modest, role when the AR pathway is active. The results of our initial studies using MDA PCa 118a and 118b cells suggested that they might have an active, highly upregulated Wnt/beta-catenin signaling pathway compared with that in PC-3 and MDA PCa 2b cells, which are 2 other bone-derived PCa cell lines. Briefly, in our original comparative gene-array study (Human Genome U133A microarray, Affymetrix) of MDA PCa 118a and 118b, MDA PCa 2b, and PC-3 cells, we found that the fibroblast growth factor (FGF) axis mediated the osteoblastic progression of these cells in bone (4). This comparison also revealed greater expression of several genes downstream of the canonical Wnt/beta-catenin pathway, including *FGF18*, immunoglobulin transcription factor-2 (*ITF2*; also alled *TCF4*), neuronal cell adhesion molecule (*NrCAM*), SRY-related HMG-box 2 (*SOX2*), and bone morphogenetic protein 4 (*BMP4*), in the MDA PCa 118a and 118b cells [Wnt-canonical target genes were from " The Wnt homepage" (5) and from a recent publication (6)].

The protein beta-catenin has at least 2 functions of interest in PCa: it participates in cadherin-mediated adhesion, and it is the "molecular node" of the Wnt canonical signaling pathway. In the absence of Wnt signals (i.e., when the pathway is inactive), the serine/threonine kinase glycogen synthase kinase 3 b (GSK3b) forms complexes with adenomatous polyposis coli, axin/conductin, and casein kinase 1 proteins, which in turn bind to soluble beta-catenin and facilitate its phosphorylation at codons 29, 33, and 37 (containing serine residues) and codon 41 (containing threonine residues). Phosphorylated beta-catenin then binds the E3 ubiquitin ligase beta-TrCP and undergoes proteosomal degradation, preventing the accumulation and transcriptional activity of beta-catenin. When Wnt ligands bind their receptor complex, the resulting activation of the cytoplasmic protein disheveled inactivates GSK3b, thereby preventing degradation of soluble beta-catenin and stabilizing it in the cytoplasm (7). Cytoplasmic beta-catenin then translocates to the nucleus, where it heterodimerizes with transcription factors of the T-cell factor/lymphoid enhancer–binding factor (TCF/LEF) family (8–10). Those heterodimers then bind to DNA and activate the expression of specific genes (11, 12). Accumulation of soluble beta-catenin is therefore critical for activation of Wnt transcription in the pathway.

Previous studies implicated beta-catenin in the pathogenesis of PCa because it localizes in tumor-cell nuclei in 20% to 40% of CRPC specimens (13–15). More recently, another group reported that activation of Wnt/beta-catenin signaling is involved in PCa initiation and progression in a mouse model (16, 17). Together, these findings imply that the Wnt canonical pathway is involved in the pathogenesis of a subgroup of advanced PCas.

Beta-catenin may also act as a coactivator of the AR (18), and it has been proposed that the AR competes with TCF/LEF transcription factors for beta-catenin, thus interfering with beta-catenin–TCF/LEF signaling (19). However, because the MDA PCa 118b tumor line does not express AR (4), the activation of beta-catenin in this model cannot involve that interaction. Therefore, the purpose of this study was to use the AR-null MDA PCa 118b cells to identify downstream target genes of Wnt/beta-catenin signaling in PCa.

## Materials and Methods

### Cell cultures, mutant beta-catenin generation, and Western blot analysis

Human MDA PCa 2b cells (20) were propagated in BRFF-HPC1 medium (Athena Enzyme Systems) with 20% FBS (Sigma-Aldrich). The PCa cell lines PC-3 and LNCaP, obtained from the American Type Culture Collection, were maintained in RPMI 1640 medium (GIBCO Invitrogen) with 10% FBS. Short-term cultures of MDA PCa 118b PCa cells (4) were isolated from subcutaneous tumors developed in SCID mice (Charles River Laboratories). Briefly, the tumors were digested in Accumax cell-disaggregation solution (Innovative Cell Technologies), filtered through a 70-micron cell strainer and then separated using a Ficoll gradient solution. These cells were then cultured in CnT52 medium (Millipore) in petri dishes or in 6-well plates coated with FNC coating mix (Athena Enzyme Systems).

D32G-mutant beta-catenin was generated by nucleotide substitution in wt human beta-catenin (a gift from Dr. P. McCrea, Department of Biochemistry and Molecular Biology, The University of Texas MD Anderson Cancer Center) with the use of a QuikChange site-directed mutagenesis kit (Stratagene Agilent). The mutant was confirmed by direct sequencing. Wild-type (wt) and D32G-mutant human beta-catenin were subcloned into p3XFLAG-CMV-7.1 expression vector (Sigma-Aldrich).

Western blotting was performed following standard procedures. The Flag epitope of p3XFLAG-CMV-7.1 expression vector and beta-catenin were detected after incubation with anti-Flag (monoclonal anti-Flag M2-peroxidase; Sigma-Aldrich) or mouse anti–beta-catenin (BD Transduction Laboratories) antibodies.

### Immunocytochemical and immunohistochemical analyses

For immunocytochemical analysis, MDA PCa 118b, PC-3, and MDA PCa 2b cells grown on tissue culture slides were immunostained with antibodies to beta-catenin (BD Biosciences) and then with an anti-mouse secondary antibody labeled with Alexa 594 dye; counterstaining was with DAPI.

Using a Leica TCS Sp5 spectral confocal microscope, we captured immunofluorescent images in which beta-catenin was detected at 590-nm excitation and 618-nm emission, and DAPI, at 360-nm excitation and 460-nm emission.

For immunohistochemical analysis, tissue sections (4 μm thick) were treated with Target Retrieval Solution (Dako) and stained with anti–beta-catenin (1:100 dilution; Zymed Laboratories) or anti-AR (1:50 dilution; Dako) antibodies. The slides were counterstained with Mayer’s hematoxylin (Poly Scientific R & D).

### Real-time reverse-transcription (RT)-PCR, beta-catenin knockdown, and gene-expression analyses

The relative mRNA level for each gene was quantified by using real-time RT-PCR with SYBR Green (Applied Biosystems Life Technologies) and a Stratagene Mx3000P quantitative PCR (qPCR) system (Applied Biosystems). cDNA was prepared by using TaqMan RT reagents (Roche Applied Biosystems). Gene-specific primers used for cDNA amplification are listed in Supplementary Table 1.

To knock down beta-catenin in MDA PCa 118b cells, the cells were transiently transfected with a validated beta-catenin–specific small interfering RNA (siRNA) (b-cat-si; s438, Ambion Applied Biosystems) and, as a control, a nontargeted siRNA (control-si), by using a Nucleofector kit (Amaxa Lonza). Forty-eight hours after their transfection, cells were collected to isolate total RNA by using an RNeasy mini kit (Qiagen). cDNA was subsequently prepared for comparative gene-array analysis (HuGene 1.0 ST; Affymetrix). The analysis was performed in quadruplicate on all preparations.

### Animals, intrabone injections, and bone tissue sample processing

All animal experiments were conducted in accordance with accepted standards of humane animal care. Six 6- to 8-week-old intact male CB17 SCID mice (Charles River Laboratories) were given injections into the distal end of 1 femur with control-si– and 6 mice, with b-cat-si–transfected MDA PCa 118b cells ($1 \times 10^6$) according to procedures described elsewhere (4).

Two weeks later, 6 mice were killed (3 from each group: control-si–transfected and b-cat-si–transfected MDA PCa 118b cells), and the femurs bearing MDA PCa 118b tumors were resected, fixed, and embedded in methylmethacrylate by the Bone Histomorphometry Core Facility at MD Anderson (M.W.S.). Tissue sections were stained with von Kossa stain, and Osteo II software, version 8.40.20 (Bioquant), was used to measure the ratio of bone volume to tissue volume.

Six weeks after the intrabone cell injections, the tumor burden of another 6 mice (3 from each group) was monitored indirectly by x-ray analysis. Then the marrow area shown in the x-ray film was outlined in the mice's femurs by using the NIH ImageJ software. The relative bone marrow cavity area was calculated by dividing the area in the tumor-bearing bone by the area in the non-injected bone (i.e., contralateral femur).

### TCF luciferase reporter assay and transfection

Beta-catenin–mediated transcription was evaluated by using 2 different promoter–reporter constructs. We used a TOP-flash reporter gene construct containing 4 consensus TCF binding sites (21). A FOP-flash construct with a mutated TCF binding site was used as a negative control.

MDA PCa 118b, PC-3, and MDA PCa 2b xenograft tumors were harvested, made into single-cell suspensions, and plated to grow to 60% confluence. After 24 hours, cells were transfected with Lipofectamine 2000 (Invitrogen) plus 2 μg of the TOP-flash reporter or the FOP-flash control construct. Transfected cells were harvested 24 hours later. *Renilla* was used as a co-reporter vector to normalize transfection efficiency. Reporter assays were done by using a luciferase reporter system (Promega).

### Human PCa bone metastasis specimens

We tested 27 archived samples from PCa bone metastases selected from a tissue bank supported by the NIH prostate cancer SPORE grant at MD Anderson. All specimens had

been obtained after the patients had provided written informed consent for the use of their tissues, according to an IRB-approved protocol. All sections were from formalin-fixed, paraffin-embedded tissue specimens; specimens had been decalcified in formic acid. For beta-catenin immunostaining, sections were classified according to the percentages of cells with positive nuclear, cytoplasmic, and membranous staining. For AR, we scored the percentage of cells showing positive nuclear immunostaining. Slides were read independently by 2 investigators (V.T. and N.M.N.); evaluations were concordant in 90% of the readings. Differences were resolved by consensus after joint review.

### Statistical analyses

Correlations between beta-catenin nuclear localization and AR expression were analyzed by using Fisher's exact test. Two-sample *t* tests for equal variance were used to identify differences between the means of the different treatment groups. Statistical significance was set at $P < 0.05$.

## Results

### Comparative gene-expression and immunohistochemical analyses reveal active beta-catenin/TCF signaling in MDA PCa 118b cells

Real-time RT-PCR analysis showed that *FGF9*, *BMP4*, *ITF2*, *NrCAM*, and *SOX2* expression was greater in MDA PCa 118b than it was in PC-3 xenografts. The expression patterns of these genes were similarly higher in MDA PCa 118b than in MDA PCa 2b xenografts. *AR* was highly expressed in only the MDA PCa 2b xenografts. Collectively, these findings (summarized in Table 1) suggest that beta-catenin–Wnt signaling is upregulated in MDA PCa 118b cells.

Beta-catenin was localized in both the cytoplasm and nucleus of the MDA PCa 118b cells but was present in only the membrane of the MDA PCa 2b and PC-3 cells, as assessed by immunohistochemical staining of the cells growing subcutaneously in SCID mice (Fig. 1A). We confirmed the nuclear localization of beta-catenin in MDA PCa 118b cells on confocal microscopy (Fig. 1B).

We found high basal levels of TOP-flash reporter transactivation in MDA PCa 118b cells but not in MDA PCa 2b or PC-3 cells (Fig. 1C). Thus, these findings, together with those showing beta-catenin nuclear localization in MDA PCa 118b cells, suggest that the Wnt canonical pathway is active and highly upregulated in these cells.

### MDA PCa 118b and MDA PCa 118a cells contain mutant beta-catenin

We analyzed the sequence of the beta-catenin gene and found that MDA PCa 118b cells have a mutation in codon 32, with GAC changed to GGC, i.e., aspartic acid (D) substituted for glycine (G). Codon 32 lies within the consensus recognition motif for ubiquitination of beta-catenin, so mutations at codon 32 alter ubiquitination and result in transformation of cells expressing this mutation (22, 23). We also analyzed the status of beta-catenin in MDA PCa 118a cells, which are derived from a different bone metastasis from the same man. We found that MDA PCa 118a and 118b cells bear the same beta-catenin mutation, but no such mutations were found in the MDA PCa 2a, MDA PCa 2b, LNCaP, and PC-3 lines (data not shown).

The D32G mutation has been reported to be associated with beta-catenin nuclear accumulation in PCa (24), suggesting pathway activation. We subsequently sequenced the entire coding frame sequence of beta-catenin in MDA PCa 118b cells and confirmed that D32G is the only beta-catenin mutation. Furthermore, we obtained evidence suggesting that

MDA PCa 118b cells are heterozygous for the D32G beta-catenin mutant (Fig. 2A). These results suggest that mutation leads to stabilization of beta-catenin in MDA PCa 118b cells.

### D32G-mutant beta-catenin is a potent transcription activator

We transiently transfected MDA PCa 2b and PC-3 cells with empty vector or with wt or D32G-mutant beta-catenin and assessed TOP-flash reporter transactivation. The D32G mutant significantly induced TCF/LEF-mediated transactivation in both PCa cell lines (Fig. 2B).

Collectively, these results demonstrate that the D32G mutant can upregulate beta-catenin–TCF signaling in PCa cells.

### D32G-mutant beta-catenin induces activation of beta-catenin/TCF target genes in PCa cells

We next transiently transfected PC-3 cells with empty vector or with Flag–wt or Flag–D32G-mutant beta-catenin. Gene-expression analysis demonstrated that D32G-mutant beta-catenin stimulated increased expression of *BMP4*, *WISP*1, and *FGF9* (known downstream target genes in the beta-catenin–TCF pathway) at higher levels than wt beta-catenin (Fig. 2C), suggesting that the D32G mutant is a potent transcriptional activator. In contrast, neither D32G-mutant nor wt beta-catenin significantly changed the expression of c-Myc and cyclin D1.

We next assessed the effect of beta-catenin silencing in MDA PCa 118b cells. Transient transfection with siRNA (b-cat-si) to knock down beta-catenin in MDA PCa 118b cells significantly reduced the beta-catenin mRNA level ($P < 0.05$; Fig. 3A) as well as BMP4, WISP1, and cyclin D1 ($P < 0.01$, $P < 0.005$, and $P < 0.005$, respectively) and modestly reduced the expression of FGF9 ($P < 0.05$). These results suggest that the expression of BMP4, WISP1, and FGF9 in MDA PCa 118b cells is partially regulated by D32G-mutant beta-catenin expression, since their expression was also activated in PC-3 cells after expression of D32G-mutant but not wt beta-catenin.

To test the effect of beta-catenin knockdown in vivo, we injected b-cat-si– and control-si–transfected MDA PCa 118b cells intrafemorally into SCID mice. Two weeks after those injections, the bone volume in the distal end of the femur injected with control-si–MDA PCa 118b cells was significantly lower than it was in the femurs injected with b-cat-si–MDA PCa 118b cells ($P = 0.0268$; Fig. 3B). At 6 weeks after the injections, x-ray analysis revealed a greater bone marrow cavity area in the femurs injected with control-si–MDA PCa 118b cells than that in the femurs injected with b-cat-si–MDA PCa 118b cells ($P = 0.036$; Fig. 3C). Together, the 2- and 6–week results indicate that the tumor burden was reduced in the bones injected with b-cat-si–MDA PCa 118b cells, suggesting that beta-catenin silencing reduces the tumorigenicity of MDA PCa 118b cells. This was as expected, given the known oncogenic properties of beta-catenin. Our results also indicate that our strategy to downregulate D32G expression in MDA PCa 118b cells was successful.

To identify novel beta-catenin downstream target genes, we subsequently performed a comparative gene-array analysis (HuGene 1.0 ST; Affymetrix) between b-cat-si– and control-si–transfected MDA PCa 118b cells. Initially, the array results appeared to be highly consistent between replicates both within and between treatments. Paired *t* testing identified no genes that were expressed differently between the test and control groups. However, by using mixed linear model analysis, we identified 10 genes that were expressed differently between the control-si– and b-cat-si–transfected groups, at the false discovery rate of 0.05 (Fig. 3D). Seven of the 10 were downregulated: *CTNNB1* [intracellular beta-catenin complex (25)]; *Axin2* (a downstream target and negative pathway regulator); *HAS3* and *HAS2* [hyaluronan synthases 3 and 2; HAS2 synthesizes hyaluronan, or hyaluronic acid

(HA), a core component of the extracellular matrix (ECM) (26)]; *APCDD1* (adenomatosis polyposis coli downregulated 1); *IRF3* (interferon regulatory factor 3); and *FAM178B* (family with sequence similarity 178 member B). The other 3 were upregulated: *CCDC80* (coiled-coil domain containing 80), *AMIGO2* (adhesion molecule with Ig-like domain 2), and *SLC17A5* (solute carrier family 17, an anion/sugar transporter).

In an independent assay, we also performed gene-expression analysis by using real-time qRT-PCR and confirmed that *CTNNB1* and *Axin2* expression was downregulated in MDA PCa 118b cells transfected with b-cat-si relative to their expression in control-si–transfected cells (by 3.8 and 2.3 times, respectively). *Axin2* is a widespread Wnt-axis downstream target gene (27, 28). These results thus confirmed the successful reduction of Wnt canonical pathway activity.

### D32G-mutant beta-catenin regulates HAS2 expression

Because HA has been shown to predict biochemical recurrence of human PCa (29) and to induce tumorigenesis and metastases in experimental systems (30, 31), we selected HAS2 and HAS3 to further test the role of beta-catenin on regulation of their expression. First, we confirmed that the expression of HAS2 and HAS3 is 2.3 times lower in MDA PCa 118b cells transfected with b-cat-si relative to their expression in cells transfected with control-si (data not shown).

To further assess the effect of wt and D32G-mutant beta-catenin in HAS2 and HAS3 expression, we transiently transfected PC-3 cells with empty vector or with Flag-wt or Flag–D32G-mutant beta-catenin to establish whether that would result in activation of the Wnt/beta-catenin pathway. For that, we assessed beta-catenin protein levels and transcriptional activation of *Axin2*, a well-recognized Wnt–beta-catenin–regulated gene (27, 28). We found similar levels of beta-catenin expression in PC-3 cells transfected with wt and D32G-mutant beta-catenin, indicating the effectiveness of the transfection (Fig. 4A). Axin2 expression was significantly induced by both wt and D32G-mutant beta-catenin ($P = 0.003$ and 0.005, respectively; Fig. 4B), indicating that the Wnt canonical signaling pathway was upregulated. However, D32G-mutant beta-catenin increased the expression of Axin2 18-fold, whereas wt beta-catenin increased it by only 1.8-fold, which suggests that the D32G mutant is a more potent transactivator than the wt is or that it accumulates more efficiently in the cells' nuclei than the wt does.

When we assessed HAS2 and HAS3 expression in those transfected PC-3 cells, we found higher HAS2 expression in the PC-3 cells transfected with the D32G-mutant beta-catenin than in those transfected with wt beta-catenin or empty vector ($P = 0.007$; Fig. 4C). No HAS3 induction was observed with either mutant or wt beta-catenin (Fig. 4D). Together, these results suggest that HAS2 is a downstream target of beta-catenin in PCa cells.

### Beta-catenin and AR nuclear accumulation are inversely correlated in PCa bone metastases

To establish whether beta-catenin's accumulation in the cytoplasm and nuclei of AR-negative human PCa cells was an isolated (or low-incidence) occurrence in MDA PCa 118b cells, we stained sections from 27 archived CRPC bone metastases (excluding the case of origin of the MDA PCa 118 xenograft) with antibodies against AR and beta-catenin in consecutive sections. In accordance with previously reported results (13–15), beta-catenin nuclear staining was found in about 40% of the specimens. Additionally, we found that the sample with the highest expression of beta-catenin was negative for AR expression, a pattern similar to the one we found in MDA PCa 118b cells (Fig. 5). Furthermore, we found

a marginally statistically significant inverse association between beta-catenin nuclear localization and AR nuclear staining ($P = 0.056$, Fisher's exact test; Fig. 5).

These results suggest that the beta-catenin:AR ratio defines a subpopulation of men with PCa bone metastases.

## Discussion

The results of these studies showed that the AR-negative PCa cell line MDA PCa 118b expresses D32G-mutant beta-catenin, which results at least partially in nuclear beta-catenin accumulation and active beta-catenin–TCF signaling. We also showed—for the first time, to our knowledge—that D32G-mutant beta-catenin induces expression of HAS2, a membrane-bound synthase of HA, a major constituent of the ECM (32). Our results concur with those previously published that beta-catenin stimulates HA production and also lend support to previous observations that the transforming effects of beta-catenin depend on HA production and HA–cell interactions (33). Earlier studies also showed that increased HA production promotes anchorage-independent growth and cell invasiveness and that HA expression in PCa biopsy specimens correlates with biochemical recurrence after radical prostatectomy (29, 33). Our findings add to these by suggesting that beta-catenin–induced HAS2 plays an important role in the progression of PCa.

Abundant evidence also exists showing that activation of downstream target genes by beta-catenin–TCF complex leads to increased proliferation and decreased differentiation of epithelial cells (34). Exon 3 is the hotspot for mutation in various malignant human tumors because it contains not only the consensus sequences for multiple kinases but also a ubiquitination consensus sequence. At that exon, the most common mutations occur at serine and threonine residues Ser37, Thr41, and Ser45. Additionally, the nonphosphorylatable residues Asp32 and Gly34 rank within the top 6 mutations identified in human tumors: beta-catenin residues in the destruction motif Asp32, Ser33, Gly34, and Ser37 directly bind beta-TrCP1 (35), and mutation of Asp32 greatly reduces the ability of beta-catenin to be ubiquitinated by beta-TrCP1 without altering the ability to act as a substrate for GSK3b (36). Mutated Asp32 also mediates a transforming phenotype for growth and migration in the stable nontransformed epithelial cell line MDCK (23).

Further, the Wnt signaling pathway has previously been implicated in the progression of PCa (19). Various of the amino acid–substitution mutations located at exon 3 of beta-catenin have been found in about 5% of PCa specimens tested by several groups of investigators (24, 37, 38). For example, in 1 previous study of a codon-32 mutant of beta-catenin, D32A, in which aspartate is mutated to alanine, expression of the D32A mutant in a nontransformed epithelial cell line increased oncogenic cellular transformation. In addition, a slightly different codon-32 mutant of beta-catenin, D32G, in which aspartate is mutated to glycine, was identified in MDA PCa 118b cells and, as our results have confirmed, that mutation is associated with beta-catenin nuclear accumulation in PCa (24), suggesting that the Wnt canonical pathway is activated. Thus, although mutations in beta-catenin have been reported in only 5% of cases of PCa, the high transcription activity that results from the D32G mutant is an important tool for identifying downstream target genes in PCa.

Moreover, beta-catenin may act as a coactivator of the AR (18), and it has been proposed that the AR competes with TCF/LEF for beta-catenin, thus interfering with beta-catenin–TCF/LEF signaling (19). Our finding an inverse association between beta-catenin nuclear localization and AR expression in human PCa bone metastases supports the concept that the beta-catenin:AR ratio may help to identify different subpopulations of patients with PCa who may require different management of the disease.

It has also been reported that beta-catenin–LEF-1 signaling is activated after epithelial-to-mesenchymal transition (EMT; thought to mediate invasive and metastatic behavior during cancer progression) and that beta-catenin signaling contributes to the maintenance of EMT (39, 40). Recent reports indicate that androgens induce EMT in PCa epithelial cells and that expression levels of AR correlate inversely with androgen-mediated EMT in those cells (41). Thus, low AR content may be required for the EMT phenotype by enabling beta-catenin–LEF-1 signaling. Together, this evidence and our results suggest that activation of beta-catenin by androgen signaling serves as an alternative mechanism of androgen-induced EMT in PCa epithelial cells.

We conclude that our identification of a previously unknown downstream target gene of activated Wnt–beta-catenin, *HAS2*, combined with high nuclear localization of beta-catenin in PCa cells with little or no AR expression may define a subpopulation of men with bone-metastatic PCa whose disease requires a different form of treatment than those used in other men with PCas. This pattern of findings may thus help clinicians provide indivualized therapy for some men with advanced PCa.

## Supplementary Material

Refer to Web version on PubMed Central for supplementary material.

## Acknowledgments

We thank Dr. P. McCrea for supplying the D32G-mutant beta-catenin as well as for useful discussion, and we also thank Karen Phillips, ELS, for her excellent editorial work.

**Grant Support**

This work was supported by the United States Department of Defense grant PC073211 (N. Navone), the Prostate Cancer Foundation (N. Navone), and the NIH through MD Anderson's Cancer Center Support Grant, CA016672, and the Prostate SPORE grant, 5P50 CA140388.

## References

1. Burd CJ, Morey LM, Knudsen KE. Androgen receptor corepressors and prostate cancer. Endocr Relat Cancer. 2006 Dec; 13(4):979–94. [PubMed: 17158750]
2. Sun S, Sprenger CC, Vessella RL, Haugk K, Soriano K, Mostaghel EA, et al. Castration resistance in human prostate cancer is conferred by a frequently occurring androgen receptor splice variant. J Clin Invest. 2010 Aug 2; 120(8):2715–30. [PubMed: 20644256]
3. Watson PA, Chen YF, Balbas MD, Wongvipat J, Socci ND, Viale A, et al. Constitutively active androgen receptor splice variants expressed in castration-resistant prostate cancer require full-length androgen receptor. Proc Natl Acad Sci U S A. 2010 Sep 28; 107(39):16759–65. [PubMed: 20823238]
4. Li ZG, Mathew P, Yang J, Starbuck MW, Zurita AJ, Liu J, et al. Androgen receptor-negative human prostate cancer cells induce osteogenesis in mice through FGF9-mediated mechanisms. J Clin Invest. 2008 Aug; 118(8):2697–710. [PubMed: 18618013]
5. The Wnt home page. Stanford: 1997–2010 Roel Nusse. [Updated 2010 October; cited, 2011 November]. Wnt target genes available from http://www.stanford.edu/group/nusselab/cgi-bin/wnt/target_genes
6. Yochum GS, McWeeney S, Rajaraman V, Cleland R, Peters S, Goodman RH. Serial analysis of chromatin occupancy identifies beta-catenin target genes in colorectal carcinoma cells. Proc Natl Acad Sci USA. 2007 Feb 27; 104(9):3324–9. [PubMed: 17360646]
7. van Es JH, Barker N, Clevers H. You Wnt some, you lose some: oncogenes in the Wnt signaling pathway. Curr Opin Genet Dev. 2003 Feb; 13(1):28–33. [PubMed: 12573432]

8. Molenaar M, van de Wetering M, Oosterwegel M, Peterson-Maduro J, Godsave S, Korinek V, et al. XTcf-3 transcription factor mediates β-catenin-induced axis formation in Xenopus embryos. Cell. 1996 Aug 9; 86(3):391–9. [PubMed: 8756721]
9. van de Wetering M, Cavallo R, Dooijes D, van Beest M, van Es J, Loureiro J, et al. Armadillo coactivates transcription driven by the product of the Drosophila segment polarity gene *dTCF*. Cell. 1997 Mar 21; 88(6):789–99. [PubMed: 9118222]
10. Behrens J, von Kries JP, Kühl M, Bruhn L, Wedlich D, Grosschedl R, et al. Functional interaction of β-catenin with the transcription factor LEF-1. Nature. 1996 Aug 15; 382(6592):638–42. [PubMed: 8757136]
11. He T-C, Sparks AB, Rago C, Hermeking H, Zawel L, da Costa LT, et al. Identification of c-*MYC* as a target of the APC pathway. Science. 1998 Sep 4; 281(5382):1509–12. [PubMed: 9727977]
12. Tetsu O, McCormick F. β-Catenin regulates expression of cyclin D1 in colon carcinoma cells. Nature. 1999 Apr 1; 398(6726):422–6. [PubMed: 10201372]
13. Chesire DR, Ewing CM, Gage WR, Isaacs WB. *In vitro* evidence for complex modes of nuclear β-catenin signaling during prostate growth and tumorigenesis. Oncogene. 2002 Apr 18; 21(17): 2679–94. [PubMed: 11965541]
14. de la Taille A, Rubin MA, Chen M-W, Vacherot F, de Medina SG, Burchardt M, et al. β-Catenin-related anomalies in apoptosis-resistant and hormone-refractory prostate cancer cells. Clin Cancer Res. 2003 May; 9(5):1801–7. [PubMed: 12738737]
15. Yardy GW, Brewster SF. Wnt signalling and prostate cancer. Prostate Cancer Prostatic Dis. 2005; 8(2):119–26. [PubMed: 15809669]
16. Yu X, Wang Y, DeGraff DJ, Wills ML, Matusik RJ. Wnt/β-Catenin activation promotes prostate tumor progression in a mouse model. Oncogene. 2011 Apr 21; 30(16):1868–79. [PubMed: 21151173]
17. Yu X, Wang Y, Jiang M, Bierie B, Roy-Burman P, Shen MM, et al. Activation of β-catenin in mouse prostate causes HGPIN and continuous prostate growth after castration. Prostate. 2009 Feb 15; 69(3):249–62. [PubMed: 18991257]
18. Terry S, Yang X, Chen M-W, Vacherot F, Buttyan R. Multifaceted interaction between the androgen and Wnt signaling pathways and the implication for prostate cancer. J Cell Biochem. 2006 Oct 1; 99(2):402–10. [PubMed: 16741972]
19. Verras M, Sun Z. Roles and regulation of Wnt signaling and β-catenin in prostate cancer. Cancer Lett. 2006 Jun 8; 237(1):22–32. [PubMed: 16023783]
20. Navone NM, Olive M, Ozen M, Davis R, Troncoso P, Tu SM, et al. Establishment of two human prostate cancer cell lines derived from a single bone metastasis. Clin Cancer Res. 1997 Dec; 3(12 Pt 1):2493–500. [PubMed: 9815652]
21. Korinek V, Barker N, Morin PJ, van Wichen D, de Weger R, Kinzler KW, et al. Constitutive transcriptional activation by a β-catenin–Tcf complex in $APC^{-/-}$ colon carcinoma. Science. 1997 Mar 21; 275(5307):1784–7. [PubMed: 9065401]
22. Al-Fageeh M, Li Q, Dashwood WM, Myzak MC, Dashwood RH. Phosphorylation and ubiquitination of oncogenic mutants of β-catenin containing substitutions at Asp32. Oncogene. 2004 Jun 17; 23(28):4839–46. [PubMed: 15064718]
23. Provost E, McCabe A, Stern J, Lizardi I, D'Aquila TG, Rimm DL. Functional correlates of mutation of the Asp32 and Gly34 residues of beta-catenin. Oncogene. 2005 Apr 14; 24(16):2667–76. [PubMed: 15829978]
24. Chesire DR, Ewing CM, Sauvageot J, Bova GS, Isaacs WB. Detection and analysis of β-catenin mutations in prostate cancer. Prostate. 2000 Dec 1; 45(4):323–34. [PubMed: 11102958]
25. Fuerer C, Nusse R, Ten Berge D. Wnt signalling in development and disease. Max Delbrück Center for Molecular Medicine meeting on Wnt Signaling in Development and Disease. EMBO Rep. 2008 Feb; 9(2):134–8. [PubMed: 18188179]
26. Viola M, Vigetti D, Genasetti A, Rizzi M, Karousou E, Moretto P, et al. Molecular control of the hyaluronan biosynthesis. Connect Tissue Res. 2008; 49(3):111–4. [PubMed: 18661323]
27. Jho E-H, Zhang T, Domon C, Joo C-K, Freund J-N, Costantini F. Wnt/β-Catenin/Tcf signaling induces the transcription of Axin2, a negative regulator of the signaling pathway. Mol Cell Biol. 2002 Feb; 22(4):1172–83. [PubMed: 11809808]

28. Lustig B, Jerchow B, Sachs M, Weiler S, Pietsch T, Karsten U, et al. Negative feedback loop of Wnt signaling through upregulation of conductin/axin2 in colorectal and liver tumors. Mol Cell Biol. 2002 Feb; 22(4):1184–93. [PubMed: 11809809]
29. Gomez CS, Gomez P, Knapp J, Jorda M, Soloway MS, Lokeshwar VB. Hyaluronic acid and HYAL-1 in prostate biopsy specimens: predictors of biochemical recurrence. J Urol. 2009 Oct; 182(4):1350–6. [PubMed: 19683287]
30. Bharadwaj AG, Kovar JL, Loughman E, Elowsky C, Oakley GG, Simpson MA. Spontaneous metastasis of prostate cancer is promoted by excess hyaluronan synthesis and processing. Am J Pathol. 2009 Mar; 174(3):1027–36. [PubMed: 19218337]
31. Simpson MA. Concurrent expression of hyaluronan biosynthetic and processing enzymes promotes growth and vascularization of prostate tumors in mice. Am J Pathol. 2006 Jul; 169(1):247–57. [PubMed: 16816377]
32. Jiang D, Liang J, Noble PW. Hyaluronan in tissue injury and repair. Annu Rev Cell Dev Biol. 2007; 23:435–61. [PubMed: 17506690]
33. Zoltan-Jones A, Huang L, Ghatak S, Toole BP. Elevated hyaluronan production induces mesenchymal and transformed properties in epithelial cells. J Biol Chem. 2003 Nov 14; 278(46): 45801–10. [PubMed: 12954618]
34. Clevers H. Wnt/β-Catenin signaling in development and disease. Cell. 2006 Nov 3; 127(3):469–80. [PubMed: 17081971]
35. Wu G, Xu G, Schulman BA, Jeffrey PD, Harper JW, Pavletich NP. Structure of a β-TrCP1-Skp1-β-catenin complex: destruction motif binding and lysine specificity of the SCFβ-TrCP1 ubiquitin ligase. Mol Cell. 2003 Jun; 11(6):1445–56. [PubMed: 12820959]
36. Provost E, McCabe A, Stern J, Lizardi I, D'Aquila TG, Rimm DL. Functional correlates of mutation of the Asp32 and Gly34 residues of beta-catenin. Oncogene. 2005 Apr 14; 24(16):2667–76. [PubMed: 15829978]
37. Voeller HJ, Truica CI, Gelmann EP. β-Catenin mutations in human prostate cancer. Cancer Res. 1998 Jun 15; 58(12):2520–3. [PubMed: 9635571]
38. Gerstein AV, Almeida TA, Zhao G, Chess E, Shih l-M, Buhler K, et al. *APC/CTNNB1* (β-catenin) pathway alterations in human prostate cancers. Genes Chromosomes Cancer. 2002 May; 34(1):9–16. [PubMed: 11921277]
39. Eger A, Stockinger A, Schaffhauser B, Beug H, Foisner R. Epithelial mesenchymal transition by c-Fos estrogen receptor activation involves nuclear translocation of β-catenin and upregulation of β-catenin/lymphoid enhancer binding factor-1 transcriptional activity. J Cell Biol. 2000 Jan 10; 148(1):173–88. [PubMed: 10629227]
40. Li J, Zhou BP. Activation of β-catenin and Akt pathways by Twist are critical for the maintenance of EMT associated cancer stem cell-like characters. BMC Cancer 2011 Activation of β-catenin and Akt pathways by Twist are critical for the maintenance of EMT.
41. Zhu ML, Kyprianou N. Role of androgens and the androgen receptor in epithelial-mesenchymal transition and invasion of prostate cancer cells. FASEB J. 2010 Mar; 24(3):769–77. [PubMed: 19901020]

## Statement of Translational Relevance

Currently there is no curative therapy for castrate-resistant prostate cancer. We confirm here that beta-catenin nuclear accumulation occurs in about 37% of castrate-resistant prostate cancer bone metastases, and we report for the first time that HAS2 is a downstream target of beta-catenin. HAS2 expression and the beta-catenin:androgen receptor ratio may help define a subpopulation of men with prostate cancer for individualized management.

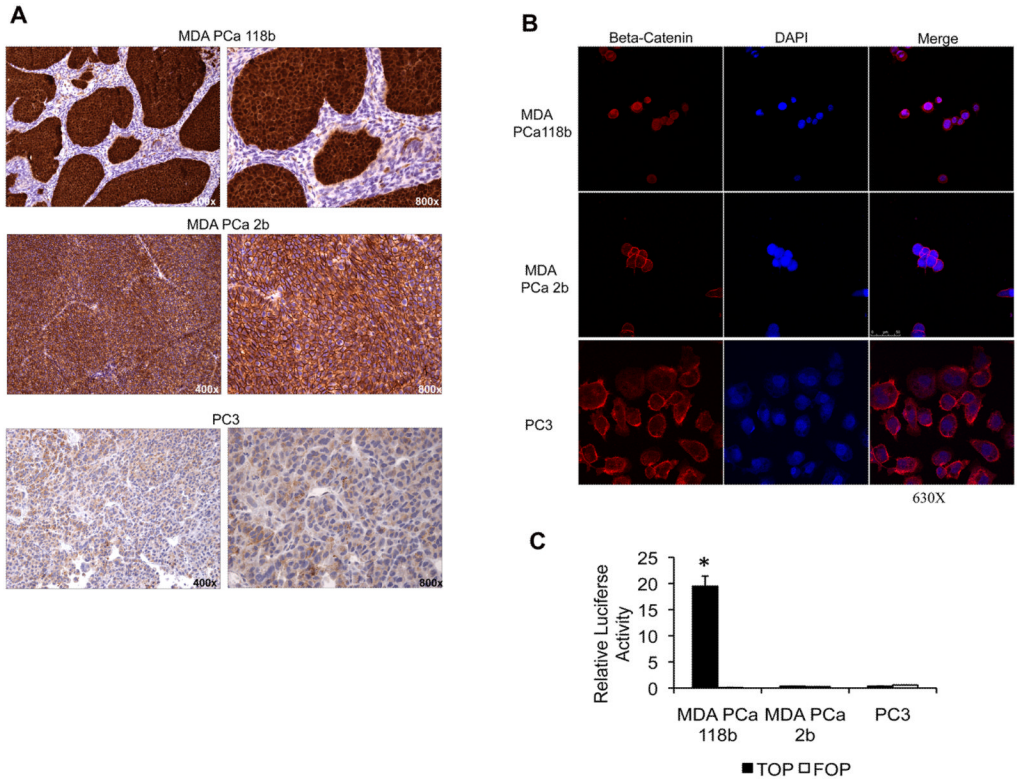


**Figure 1.**

MDA PCa 118b prostate cancer cells have an activated Wnt canonical signaling pathway. A, beta-catenin immunohistochemical staining of subcutaneous xenografts with anti–beta-catenin antibody showing strong nuclear and cytoplasmic staining on MDA PCa 118b, strong membranous staining on MDA PCa 2b, and diffuse staining on PC-3 cells. Original magnification, ×400 and ×800 on left and right panels, respectively. B, photomicrographs of those same cell lines immunostained with anti–beta-catenin antibody and visualized on confocal microscopy. Original magnification, ×630. C, transcriptional activation of TCF reporter in MDA PCa 118b, MDA PCa 2b, and PC-3 prostate cancer cells. Cells were transfected with the TOP-flash reporter or the FOP-flash control construct. *Renilla* was used as a co-reporter vector to normalize transfection efficiency. Reporter assays were performed with a luciferase reporter system. **P* < 0.001 vs. MDA PCa 118b cells transfected with the FOP-flash control construct.

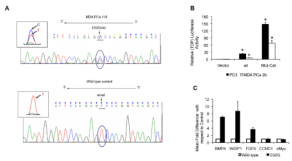

**Figure 2.**

A, beta-catenin mutation in MDA PCa 118b cells. The cDNA sequence of exon 3 in MDA PCa 118b cells growing subcutaneously in SCID mice (upper panel) shows the heterozygous T-to-C (D32G) nucleotide mutation. MDA PCa 2b cells were used as the wild-type (wt) control (lower panel). Similar results were obtained from sequencing of exon 3 of DNA extracted from the MDA PCa 118b and MDA PCa 2b cells. B, transcriptional activation of TOP-flash reporter in prostate cancer cells transfected with empty vector (vector) or with wt or D32G-mutant beta-catenin (Mut-Cat). **P* < 0.001 vs. empty vector. C, relative mRNA level of various genes 48 hours after transient transfection of PC-3 cells with wt or D32G-mutant beta-catenin. The mean mRNA levels and SDs from 3 independent reactions with each gene are expressed relative to those in cells transfected with wt control.

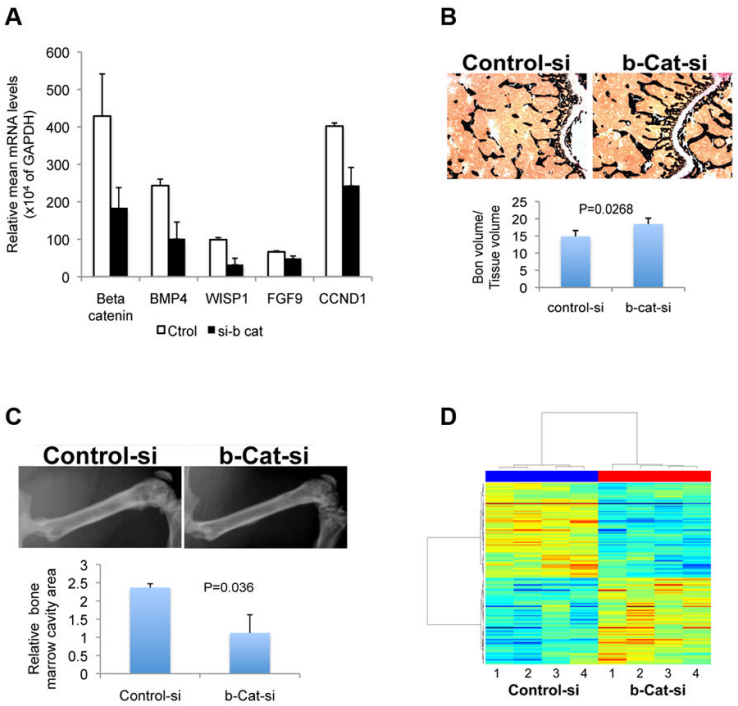


**Figure 3.**

A, the expression of selected genes in MDA PCa 118b cells with knocked-down beta-catenin. Beta-catenin was knocked down by transiently transfecting the cells with small interfering RNA (siRNA; si-b cat). As a control, the cells were transfected with non-targeted siRNA (ctrol). Gene expression was determined by quantitative RT-PCR using total RNA isolated 48 hours after transfection. B, Upper panel: representative images of sections from the distal end of femurs 2 weeks after intrabone injections with MDA PCa 118b cells transfected with control siRNA (control-si) or beta-catenin siRNA (b-Cat-si): cross sections of undecalcified bone stained with von Kossa (black). Original magnification ×400. Lower panel: ratio of bone volume to tissue volume, as assessed by bone histomorphometric analysis of the undecalcified bone sections. C, Upper panel: x-ray images of rear limbs of representative mice 6 weeks after intrafemoral injection of control-si– or b-cat-si–transfected MDA PCa 118b cells. Lower panel: relative bone marrow cavity area measured with NIH-ImageJ. D, heat map of the genes expressed differently between control-si– and b-cat-si–transfected MDA PCa 118b cells. The “lanes” labeled 1 through 4 for each siRNA are experimental replicates.

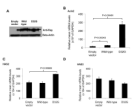

**Figure 4.**

A, Western blot analysis of lysates from PC-3 cells transiently transfected with empty vector or with wild-type or D32G-mutant beta-catenin using anti-Flag or beta-actin antibodies. Relative mRNA levels (vs. those in GAPDH) of Axin2 (B), HAS2 (C), and HAS3 (D) in PC-3 cells 48 hours after transient expression with empty vector or with wild-type or D32G-mutant beta-catenin.

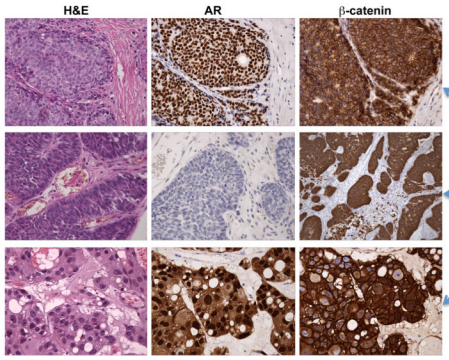


Summary of beta-catenin and AR expression in 27 human prostate cancer bone metastases

| Number of cases | B-catenin nuclear | B catenin cytopl | B-catenin membrane | AR |
|---|---|---|---|---|
| 15 | 0 | 60-100 | 100 | 60-100 |
| 1 | | 30 | 100 | 60-100 |
| 1 | 10 | 90 | 90 | 0 |
| 1 | 20 | 100 | 0 | 0 |
| 8 | 5-50 | 60-100 | 60-100 | 60-100 |
| 1 | 5 | 60 | 70 | 20 |

Beta-catenin nuclear localization and AR expression

| | AR >70 | AR < 20 |
|---|---|---|
| B-catenin nuclear 0 | 16 | 0 |
| B-catenin nuclear 5-30 | 8 | 3 |

p = 0.056 Fisher's exact test

**Figure 5.**

Immunohistochemical analysis of beta-catenin and androgen receptor (AR) in human prostate cancer bone metastases. The photomicrographs illustrate different groups of prostate cancers characterized by beta-catenin staining in the cell membrane and positive AR nuclei staining (upper panel), nuclear/cytoplasmic beta-catenin staining and no or low AR nuclear staining (middle panel), and nuclear/cytoplasmic and membranous beta-catenin staining and AR nuclear staining (bottom panel). H&E, hematoxylin and eosin staining. Original magnification ×400. The table on the right summarizes beta-catenin and AR expression in 27 human prostate cancer bone metastases, grouped according to the percentage of cells with positive staining of the markers indicated. Cytopl, cytoplasm. The table beneath the photomicrographs summarizes the number of cases with AR nuclear staining in more than 70% (AR > 70) or less than 20% (AR < 20) of the cells that also have no beta-catenin nuclear staining (B-catenin nuclear 0) and the number of those that have beta-catenin nuclear staining in 5%–30% of cells (B-catenin nuclear 5–30). $P = 0.056$ Fisher's exact test.

## Table 1

Relative mRNA levels ($\times 10^{-4}$) in various genes in different subcutaneous prostate tumor cell lines, compared with the levels in GAPDH[a]

| Gene | MDA PCa 118b | Tumor cell line PC-3 | MDA PCa 2b |
|---|---|---|---|
| *FGF9* | 863 ± 121 ⇑ | 3 ± 0.2 | Undetectable |
| *BMP4* | 1331 ± 190 ⇑ | 19 ± 4 | Undetectable |
| *ITF2* | 2783 ± 197 ⇑ | 46 ± 6 | Undetectable |
| *NrCAM* | 3581 ± 275 ⇑ | 39 ± 12 | 41 ± 5 |
| *SOX2* | 7904 ± 121 ⇑ | 59 ± 10 | 24 ± 2 |
| *OCT4* | 66 ± 6 | 62 ± 11 | 158 ± 31 |
| *AR* | Undetectable | 7 ± 2 | 2870 ± 820 |
| *Cyclin D1* | 63 ± 27 | 505 ± 193 | 823 ± 115 |
| *c-Myc* | 424 ± 57 | 1500 ± 479 | 1552 ± 336 |

[a]For each gene, data from 3 independent reactions were used to calculate the means and SDs shown. If no value in the linear range of PCR cycles of a specific RNA was detected, probably because little or no mRNA was expressed in that particular tumor sample, it was considered undetectable. Primers were human specific, and these were tested by using mRNA isolated from primary mouse osteoblasts and PC-3 cells grown in vitro. Arrows indicate the genes that are upregulated in MDA PCa 118b relative to those in both PC-3 and MDA PCa 2b cells.